Volcanic evolution of an ultraslow-spreading ridge

Håvard Stubseid (Havard.Stubseid@uib.no)
University of Bergen https://orcid.org/0000-0002-6363-1198
Anders Bjerga
University of Bergen https://orcid.org/0000-0001-5541-3898
Haflidi Haflidason
Department of Earth Science, University of Bergen https://orcid.org/0000-0002-7782-8856
Rolf Pedersen

Article

Keywords: Ultraslow-spreading ridges, volcanism, crustal accretion, hydrothermal activity

Posted Date: January 12th, 2023

DOI: https://doi.org/10.21203/rs.3.rs-2393567/v1

Additional Declarations: There is **NO** Competing Interest.

Version of Record: A version of this preprint was published at Nature Communications on July 12th, 2023. See the published version at https://doi.org/10.1038/s41467-023-39925-0.

Volcanic evolution of an ultraslow-spreading ridge

H. H. Stubseid*†, A. Bjerga*†, H. Haflidason and R. B. Pedersen

Center for Deep Sea Research and Department of Earth Science, University of Bergen, Allégaten 41, N-5007 Bergen, Norway

**Corresponding author: havard.stubseid@uib.no*

† *These authors contributed equally to this work*

Nearly 30% of the ocean crust forms at mid-ocean ridges where the spreading rate is less than 20 mm per year. According to the seafloor spreading paradigm, oceanic crust forms along a narrow axial zone, becomes inactive, and is transported away from the rift valley. However, because quantitative age data of volcanic eruptions are lacking, constructing geological models for the evolution of ultraslow-spreading crust remains a major challenge. Here, we use sediment thicknesses acquired from more than 4000 km of sub-bottom profiler data combined with C^{14} ages from sediment cores to determine the age of the ocean floor of the oblique ultraslow-spreading Mohns Ridge at the segment scale and reveal a systematic pattern of young volcanism occurring outside axial volcanic ridges. We present the first age map of a mid-ocean ridge and find that nearly half of the 6-17 km wide inner rift valley floor has been rejuvenated by volcanic activity during the last 25 Kyr. High-resolution bathymetric observations of young volcanic structures at the rift flanks indicate that crustal accretion occurs across the width of the axial valley and implies that formation of ocean crust may take more than one million years at ultraslow-spreading ridges.

Keywords: Ultraslow-spreading ridges, volcanism, crustal accretion, hydrothermal activity

Around 75% of all volcanic activity on Earth occurs at the mid-ocean ridges were tectonic plates drift apart. A central concept of seafloor spreading is that crustal accretion is confined to a narrow zone between 1-2 km in width[1-4]. According to this model, young crust appears in the central part of the rift with a linear increase in crustal age moving towards the sides[5]. However, the growth of ocean crust at the slower spreading ridges, where the magma budget is highly variable along the ridge axis, is significantly more complicated[6-8]. Direct constraints on the age and evolution of the crust at mid-ocean spreading ridges from the dating of single rock samples using U-series disequilibrium and zircon U-Pb dating[9-15], and C^{14} dating of basal sediments [16,17], have significantly increased our understanding of magmatic and tectonic processes occurring during crustal accretion. Yet, there is a lack of age data, with a resolution better than that of magnetic anomalies, from the rift valley of mid-ocean ridges that could provide a more complete view of how ocean crust accretes. To advance our understanding of the processes and timescales involved in the formation of the ocean crust, we present a segment-scale age map showing the age distribution for the last ~200 Kyr of the rift valley floor. Sediment thicknesses, calculated from more than 4000 km of sub-bottom profiler data, are converted to age by establishing accurate sedimentation rates from C^{14} dating of handpicked foraminifera in sediment cores. Our dataset reveals that the volcanic activity is not restricted to pronounced axial volcanic ridges (AVRs) but occurs throughout the width of the rift valley floor.

Oblique ultraslow-spreading along the Mohns Ridge

In this contribution, we focus on the 500 km long oblique spreading Mohns Ridge between 71.2°N and 73.5°N (Fig. 1). The ridge has a spreading rate of ~14 mm yr^{-1} [18] and a sedimentation rate of 6 cm/Ka in the rift valley (Fig. 2), providing a unique age-resolution to study volcanic processes on the millennial scale. The width of the inner valley floor varies between 6 and 17 km and the

46 crustal thickness (4 ± 0.5 km) is thinner than the global average[19]. Orthogonal spreading segments
47 are characterized by AVRs that are between 15-30 km long, and 5-10 km wide, where the volcanic
48 activity appears to be focused[20,21]. Here, large extensional faults separate the volcanically active
49 regions from tectonically dominated and sedimented areas (Fig. 1). Because of the oblique
50 spreading, individual AVRs sometimes extend across the rift valley linking up with the rift
51 bounding faults [22,23]. Segmentation of the Mohns Ridge takes the form of lateral non-transform
52 offsets (NTOs) between individual orthogonal spreading segments. These offsets range from 10 to
53 40 km and separate areas of the ridge that experience different volcanic and tectonic modes of
54 spreading.

55 **Constraining the timing and distribution of volcanism**

56 To investigate the volcanic history of the rift valley, we report the results from more than 4000 km
57 of seismic lines that were collected by autonomous underwater vehicles (AUV) carrying sub-
58 bottom profilers. The dataset covers an area of 1500 km^2 that represent approximately 25 % of the
59 inner rift valley floor of the Mohns Ridge (Fig. 1). We tracked continuous seismic lines in transects
60 perpendicular to the rift valley with a spacing of 200 to 800 m between individual lines. In areas
61 with no or very thin sediment cover (less than 30 cm) we used high-resolution bathymetry and 1-
62 m resolution backscatter data to constrain the sediment cover. Based on these data, the variable
63 thickness of hemipelagic sediment that is present on top of the volcanic basement is reported as an
64 isopach map in Fig. 1 (see supplementary for further details).

65 As we show that the hemipelagic sediment accumulates at a relatively constant rate, at least for
66 the last 50 Kyr, (Fig. 2 and supplementary), the sediment thickness reflects the age of the

underlying volcanic flows. The isopach map, accordingly, reflects the spatial-temporal evolution of volcanic activity within the rift valley.

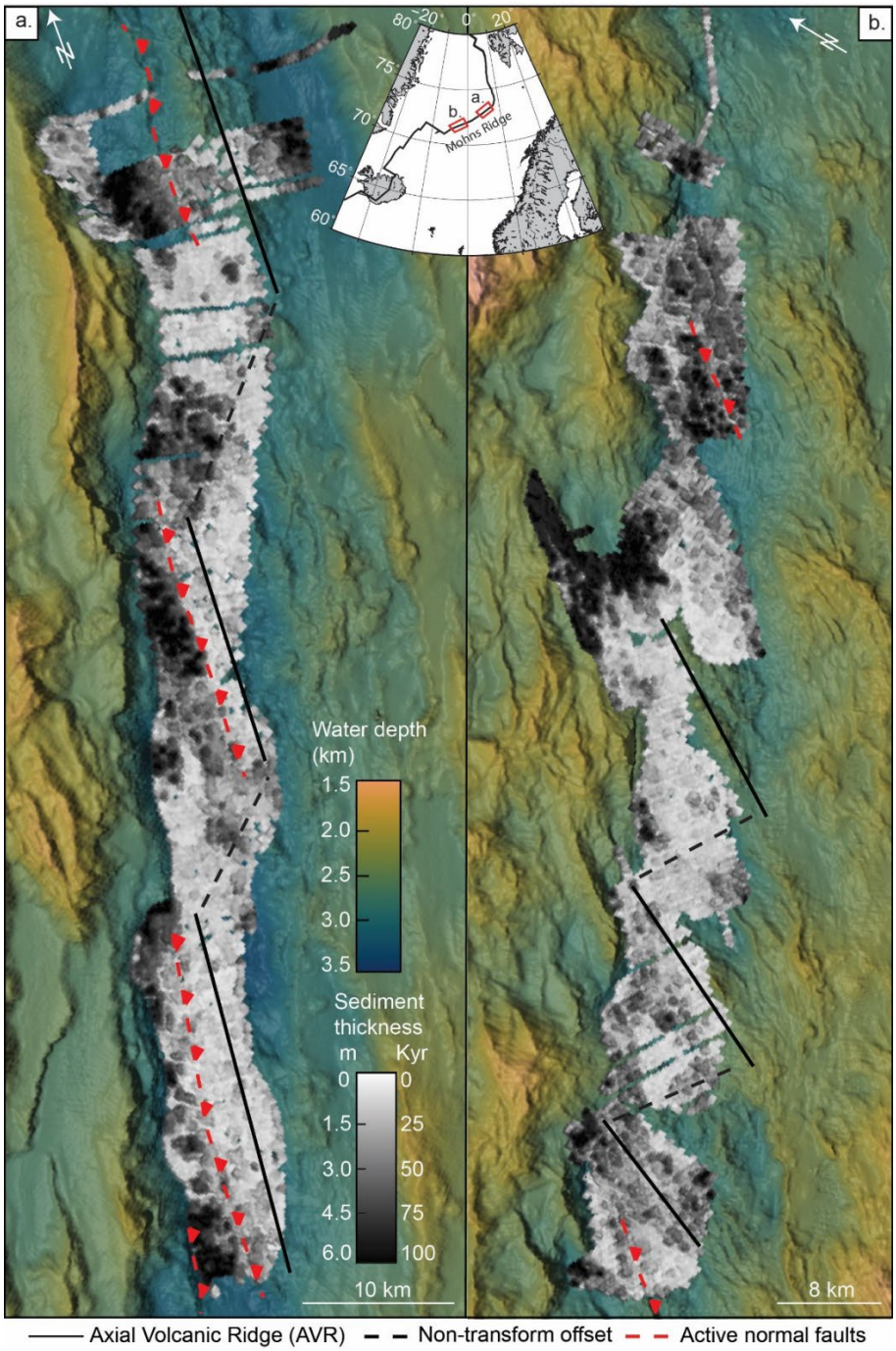

Figure 1: Distribution of sediments across the rift valley floor presented as an isopach map. The calculated sediment thickness from SBP data (grey scale) is gridded at 175 m resolution and draped onto 70 m resolution bathymetry of the rift valley. The greyscale indicates the thickness of sediments and corresponding age of the underlaying lava flows based on the acquired sedimentation rate (Fig. 2 and supplementary). Dark lines show the size and orientation of individual AVRs. Red dashed lines indicate the active normal faults and black dashed lines are the non-transform offsets in between orthogonal spreading segments. **a.** represents the northernmost part of the surveyed area, whereas **b.** is the southern segment of the ridge.

To constrain the time dimension, sedimentation rates have been calculated along the entire length of the study area (Fig. 2 and supplementary) by C^{14} dating of forams from 5 sediment cores and chemo stratigraphic correlation with the remaining 16 cores. The average sedimentation rate in the rift valley (6 cm/Kyr) is nearly 6 times of that reported in the equatorial part of the Mid-Atlantic Ridge [24]. The high sedimentation rate allows for an unprecedented high-resolution age correlation across the rift valley. The seismic acquisition parameters had a vertical resolution of approximately 30 cm, yielding an age resolution of close to five thousand years at the time-averaged sedimentation rates.

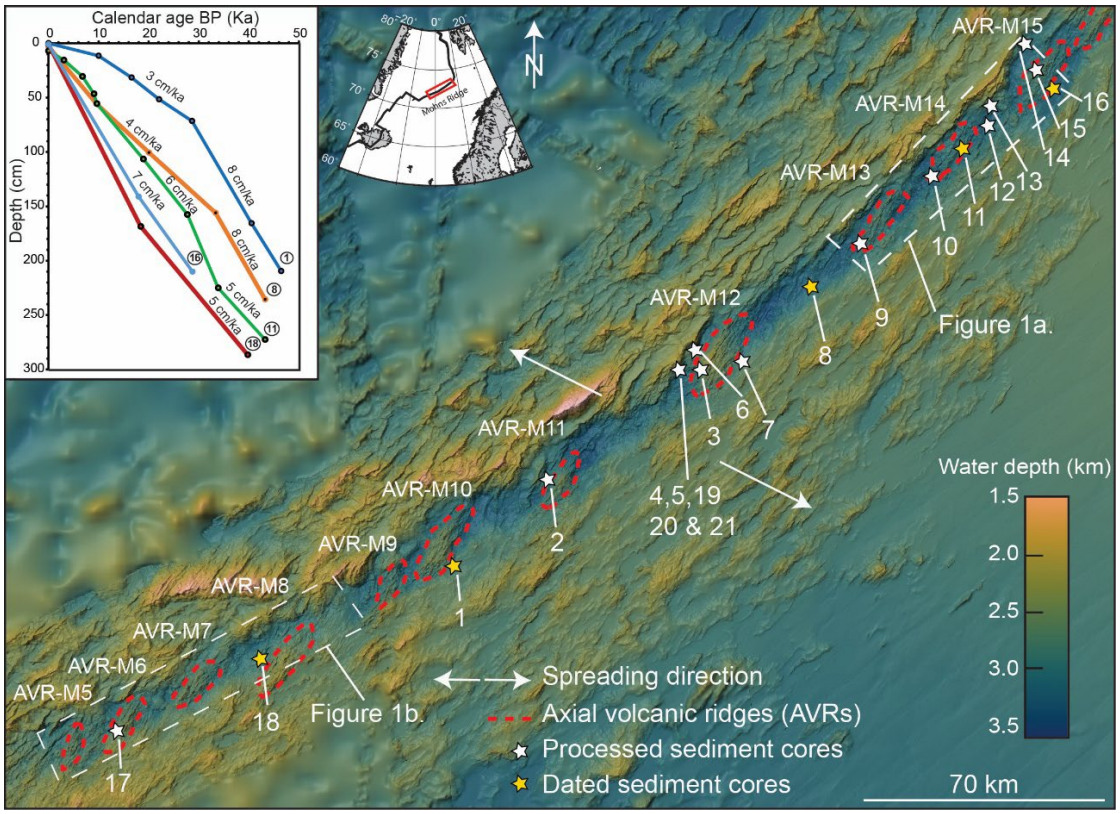

Figure 2: Overview of collected sediment cores and calculated sedimentation rates. All the collected sediment cores during the 2020 and 2021 cruise are marked as stars on a 70 m resolution bathymetry with 2 times vertical exaggeration. Yellow stars are cores that have been dated and white stars are cores that are photo-scanned and analyzed using XRF element scanning. Their chemo stratigraphy has been correlated with all other cores to strengthen the age model (details in supplementary). The outline of all AVRs is marked with a red dashed line and numbered accordingly to their location along the Mohns Ridge. Inset in the upper left corner show the sedimentation rate for each of the dated core, with a number corresponding to the location on the map (see Table S1 in supplementary). The average sedimentation rate is estimated to 6 cm/Kyr for the entire rift valley.

Spatial-temporal volcanic evolution of the rift valley

The isopach map demonstrates that 45% of the studied area is covered with less than 1.5 m of sediments, corresponding to a maximum age of 25 Kyr for the top lava flows present under the sediment cover. Our observations document that nearly half of the rift valley floor has been renewed and reshaped by volcanism during the last 25 Kyr. The sediments on top of the lavas rarely exceeds 9 m, and only locally reaches 11 m corresponding to a maximum age of 180 Kyr. This suggests that within the rift valley the upper lava flows of the volcanic basement are rarely older than 180 Kyr.

We define a total of 16 AVRs, as pronounced bathymetric highs, along the Mohns Ridge. These volcanic structures comprise 30% of the rift valley floor and have an average surface area of 125 km^2. A total of 7 AVRs have been surveyed as part of this study. Only one of the AVRs (AVR-M5) is interpreted to be volcanically extinct as the isopach map shows an average sediment thickness of 2-3 m, corresponding to an average age of 30-50 Kyr, for the entire surface of the structure (Fig. 1). All other surveyed AVRs exhibit a surface with sediment cover below 1.5 m indicating a volcanic surface younger than 25 Kyr. Calculations (Fig. 3) shows that nearly 70% of the total AVR surfaces surveyed in this study is younger than 25 Kyr. The abundance of thicker sediments is rapidly decreasing, and sediment thicknesses above 3 m are nearly absent at AVRs. The isopach map, AUV back-scatter data and ROV ground truthing support ages from 25 Kyr to present day, suggesting that these AVRs are still volcanically active. Individual volcanic centers can be seen in the isopach map as small, isolated fields with varying sediment cover leaving a patchy age pattern (Fig. 4). The volcanic structures forming this patchy pattern have an average size of ~1-2 km^2 and represent the "unit cell" of the volcanic sequence. High resolution AUV and ROV based mapping of individual AVRs show that these fundamental volcanic construction form

by multiple eruptive events with each isolated eruption covering an average area of 0.025 km^2 with lava (HHS, AB, HH & RBP in prep.).

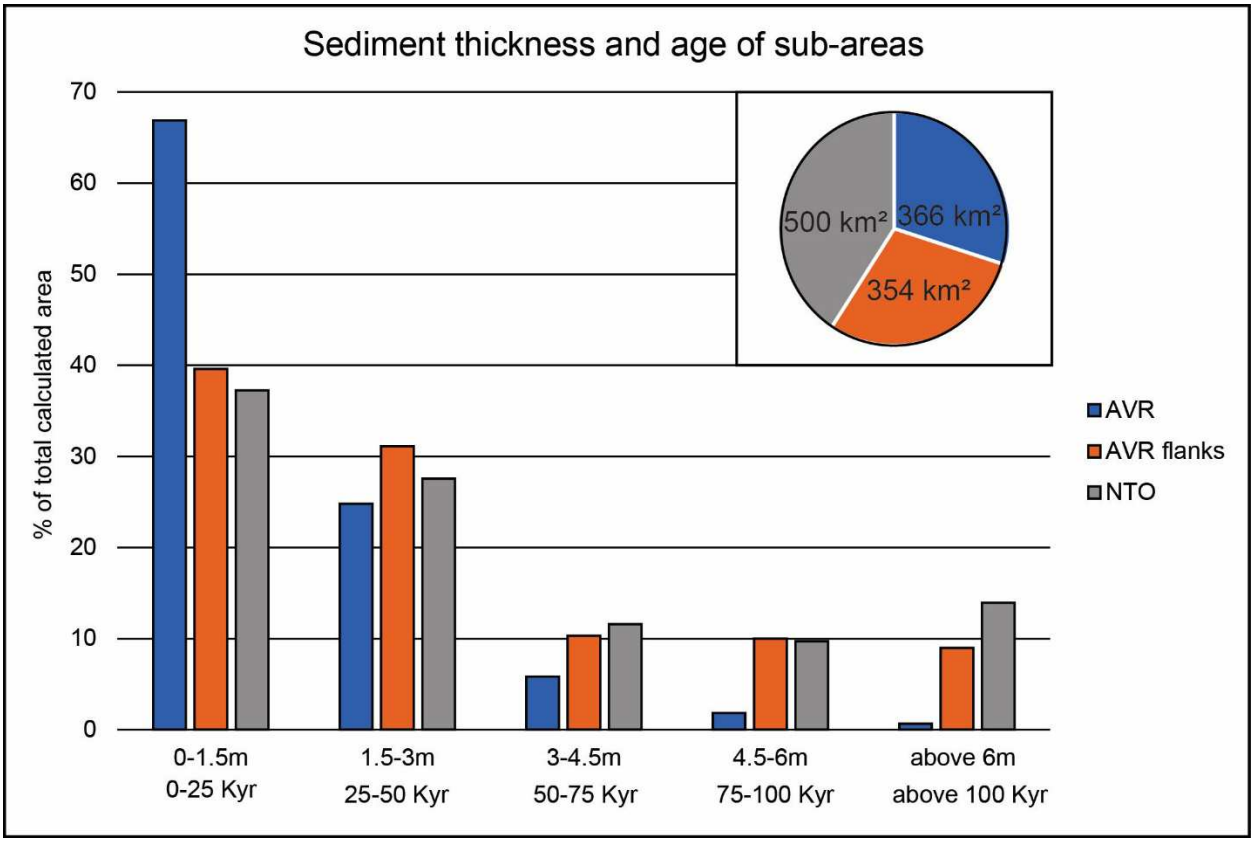

Figure 3: Variation in sediment thicknesses within different sub-areas of the rift valley. The figure summarizes the sediment thicknesses within three distinct sub-areas: axial volcanic ridges (AVR), deep areas flanking the AVRs (AVR flanks), and non-transform offsets (NTO). The ages of the volcanic basement within these sub-areas are estimated using the average sedimentation rate (Fig. 2). Calculations were done using a grey scale image, with a shade of grey for each 1.5 m sediments intervals, and the image analyses program ImageJ. All areas with sediments above 6 m are within the same class. Pie chart in the upper right corner illustrate the sizes of the sub-areas. See supplementary for further details.

The isopach map also shows that the volcanic activity is partly controlled by major normal faults that nucleates at the AVRs, for later to develop into the major fault systems that define the rift valley. The faults appear to inhibit or cut off the volcanic activity on the footwall-side of the faults (Fig. 1). For example, at AVR M-14 (Fig. 4), the isopach map reveals a volcanically active zone, 4 to 5 km wide on the central part of the AVR, limited to the west by an active normal fault and a volcanically inactive area covered in 4-6 m of sediments.

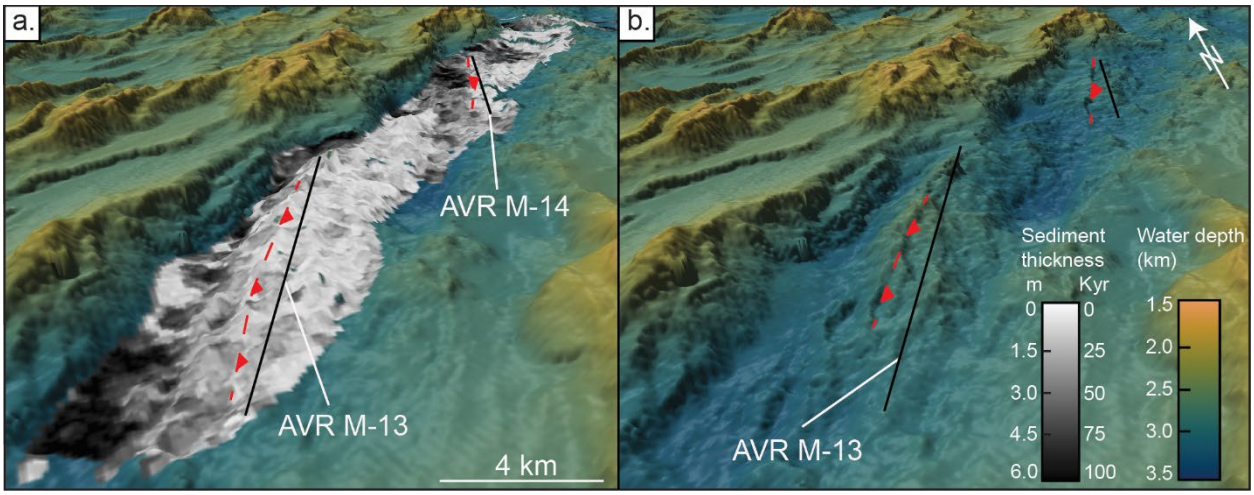

Figure 4: Detailed overview of the distribution of volcanism in the rift valley of the Mohns Ridge. a. Bathymetric map (70-m resolution) of the northern part of the Mohns Ridge with sediment thickness from sub-bottom profiler data, gridded to 175 m, draped on top of the bathymetry shown in oblique view. Greyscale show the measured sediment thickness and is converted to age based on the sedimentation rate (Fig. 2). White to light grey are areas with the youngest top lava flows and darker parts are more heavily sediments (6 m or more). Black lines indicate the size and orientation of AVRs. A patchy pattern seen on AVR M-13 is interpreted to represent the "unit cell" of the volcanic sequence. Active normal fault on both AVRs show a young volcanic terrain to the east and an older and more sedimented terrain to the west. **b.** Bathymetry (70-m resolution) in oblique view without any sediment thickness, from the same area as Fig. 3a. The bathymetry is used to further illustrate the volcanic terrain of the rift valley floor and to show the size and architecture of AVRs.

The oldest volcanic seafloor is found in the deep parts of the rift valley that flank the AVRs, or within NTOs. Locally the volcanic seafloor is here covered by up to 11 m of sediments, corresponding to an age of 180 Kyr. Here, the isopach map also reveals the patchy volcanic pattern like that seen on the AVRs. The areas flanking the AVRs and the NTOs show a similar age pattern (Fig. 3), different from the AVRs. The sediment thicknesses reveal a large age span with average ages of 35 Kyr and 50 Kyr, respectively. Calculations show that thicker sediments (from 3 m to more than 6 m) are more abundant than on AVRs (Fig. 3). The sediment stratigraphy (see supplementary) indicates steady hemipelagic sedimentation, without any major gravity flows disturbing the sedimentation rate in the deeper areas, and therefore supports the older ages. However, young volcanic constructions are common also in these areas and approximately 40% of both AVR flanks and NTOs are younger than 25 Kyr (Fig. 3). These young volcanics occurs all

the way from the foot of the AVRs to the bounding faults of the inner rift valley - where young lava flows have ponded against the major faults, extruded on top of the footwall (Fig. 5), and locally been uplifted as rider blocks. The isopach map reveals that for the volcanic seafloor that formed during the last 25 Kyr, as much as 50% formed outside the AVRs.

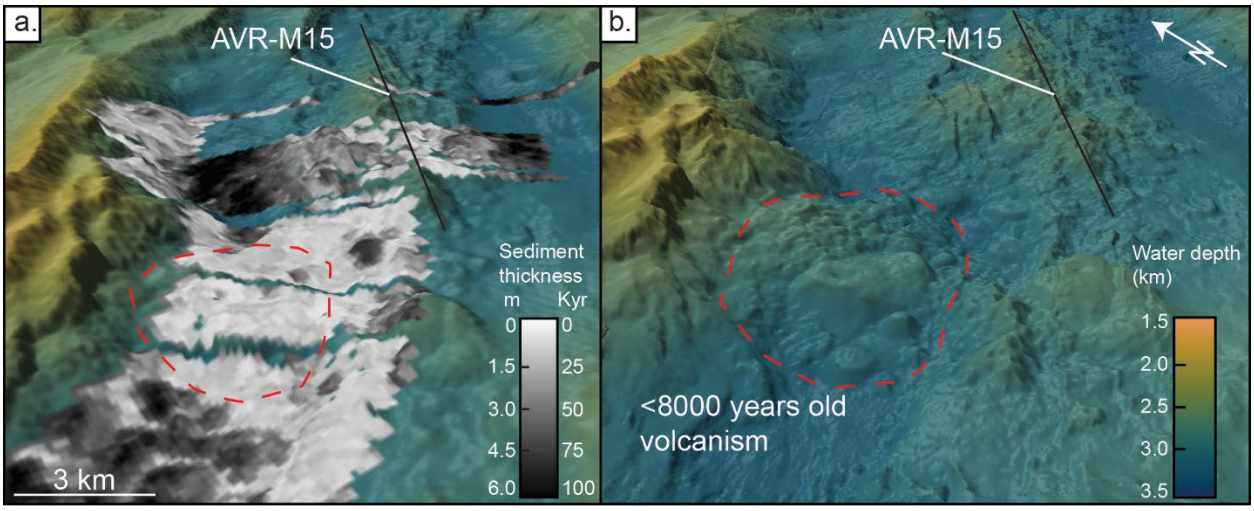

Figure 5: Example of recent volcanism at the rift bounding fault. a. Sediment distribution and age of the volcanic crust for the northernmost part of the surveyed area. The sediments clearly demonstrate a young terrain up against the fault zone, with older and more sedimented seafloor both to the north and south. Black line indicates the size and orientation of AVR. Figure shown in oblique view. **b.** High-resolution ship bathymetry (15 m resolution), with 2 times vertical exaggeration, for the same area as in Fig. 5a. The bathymetry highlights the volcanic terrain and clearly demonstrates the construction of circular volcanoes (1-2 km in diameter) and a hummocky terrain produced from a primary eruptive vent extruding at the foot wall of the rift bounding fault.

Age evolution of ultraslow-spreading mid-ocean ridges

The distribution of sediments together with high-resolution bathymetry, backscatter, and visual ROV observations along the Mohns Ridge provides quantitative age constraints for the volcanic seafloor and shows that volcanism occurs across the width of the rift valley floor (Fig. 1 and Fig. 5). The observed width of the volcanically active zone, here defined as the zone of volcanism

younger than 25 Kyr, varies from 2 to >10 km along the ridge. This is wider than the 1-2 km wide spreading axis observed at a segment of the Mid-Atlantic Ridge[2]. There, the spreading axis is defined as the area of active erupting fissures (primary eruptive vents) fed by underlying dikes, and eruptions occurring outside the spreading axis are interpreted to represent secondary vents with lava transport through tubes and channels [2] .

Along the AVRs at the Mohns Ridge, we see no sign of systematic age patterns that could support volcanic accretion along a relative narrow zone and that the volcanic seafloor gets gradually older away from such a spreading axis. Close to the AVRs, we can-not exclude that eruption may be secondary and fed by lava transported down-slope through tubes and channels. But, far away from the AVRs, at NTOs and in deep areas next to the rift valley inner bounding faults (Fig. 5), a source from local magma feeding systems seems more likely [7,8,25].

Furthermore, given a spreading rate of 14 mm/yr [18] and a width of the inner rift valley floor of ~10-15 km, the age of the crust near the rift valley inner bounding faults should be around 1 Myr on average. In contrast, our isopach map (Fig. 1) reveals that the age of the uppermost lava flow along the rift valley floor of the Mohns Ridge rarely exceeds 180 Kyr. Within the bounds of our dataset, the entire surface has been renewed by volcanic activity since Marine Isotopic Stage 6 (MIS 6). This means that the top lava flow within the rift valley is much younger than the "crustal age" predicted based on the linear spreading of the plates at constant rates and a narrow axial-centric spreading axis [2,15]. By extrapolating our dataset to the entire rift valley of the Mohns Ridge, it becomes clear that approximately half the inner rift valley floor has been renewed by volcanism during the last ~25 Kyr. Therefore, factors other than spreading rate may be important in determining the production and renewal of oceanic crust at the slowest-spreading ridges [26,27].

184 At the Mohns Ridge, it therefore appears that the crust forms by one million years of magmatic
185 activity. The intrusive sections should accordingly display such an age range. In a nearby off-axis
186 core complex, where the lower crust is exposed, we have recently documented 1.5 million years
187 of magmatism by applying U-Pb geochronology on zircons from several generations of gabbroic
188 intrusions and Ar-Ar dating on cross-cutting basaltic dikes (A. Bjerga, H.H. Stubseid, L.E.R
189 Pedersen, F. Corfu, M. Whitehouse & R. B. Pedersen, in prep.).

190 Volcanic activity is the main driver for hydrothermal activity, and active hydrothermal vent fields
191 have been discovered from within the rift valley of all slow and ultraslow-spreading ridges [28-33].
192 These vent fields support diverse and unique faunas and are associated with potentially economic
193 valuable mineral deposits. Slow and ultraslow-spreading ridges are generally suggested to sustain
194 long-lived hydrothermal systems and produce the largest mineral deposits [28,34-36]. However, the
195 rapid and widespread volcanic surface renewal documented in this study place constraints on the
196 preservation of mineral deposits on the seabed. From an economic geology perspective, we
197 therefor suggest that mineral deposits that form at the inner rift valley floor are likely to be buried
198 underneath lavas making them difficult to detect and even harder to exploit.

199 Volcanic rejuvenation of the oceanic seafloor at mid-ocean ridges is both a constructive and
200 destructive event that has important implications for many aspects of ridge accretion. The
201 determination of volcanic seafloor ages from sediment thickness along the Mohns Ridge greatly
202 expands our understanding of spreading dynamics along the slowest spreading ridges of the global
203 ridge system. We argue that the pattern of volcanism and crustal accretion presented here is
204 representative of larger parts of the global ridge system with several interesting consequences for
205 the understanding of ultraslow spreading-ridge environments. First, crustal accretion occurs on a
206 longer timescale than previously believed[2,11,12,37]. Hence, axial-centric spreading models do not

accurately describe crustal accretion at ultraslow spreading ridges[15]. Second, primary eruptive vents occur within the entire width of the rift valley floor. This suggest that the spreading axis is not only defined by the AVRs, but that spreading events and volcanism can occur anywhere within the rift valley. Third, young volcanism is widely distributed through numerous small eruption cells. Consequently, the number of volcanic eruptions may be underestimated at slow-and ultraslow-spreading ridges [38]. Fourth, exploitation for mineral deposits that do not consider the rapid and widespread surface renewal will likely overestimate the availability of mineral deposits at the seafloor. Finally, our contribution provides, for the first time, an age map of the rift valley floor of an entire ridge segment and reveal that volcanism is widely distributed in time and space at ultraslow-spreading ridges.

Supplementary Information

Supplementary information accompanies this paper in a separate file.

Acknowledgement

The crew on RV G.O. Sars and the Ægir6000 ROV-team are acknowledged for their assistance during a series of cruises. We thank Jarle A. Vikebø, Stig Monsen, Rasmus Rikter-Svendsen, Markus Mila, Lubna S. J. Al-Saadi and Heidrun M. Sande for contributions to data and sample processing, and Thibaut Barreyre, Leif-Erik R. Pedersen, and Ryan Portner for valuable feedback on previous drafts of the manuscript. The Norwegian Petroleum Directorate shared acoustic data for the study. Funding was provided through a grant to Centre for Deep Sea Research from the K.G. Jebsen and the Trond Mohn Foundations.

Availability of data and materials

All acoustic data used in this study is available at the Norwegian Petroleum Directorate at: https://npd.maps.arcgis.com/apps/webappviewer/index.html?id=cfc3c31304fe4eb8974b7d3a4bbf8c4d

All C^{14} ages used in the study is available in Supplementary Information.

Author contributions

RBP and HHS designed the study with input from AB and HH. RBP secured data and funding for the project. HHS and AB interpreted acoustic data. HH lead the processing of sediment cores and handled C^{14} dating. HHS and AB wrote the manuscript with input from HH and RBP.

References

1 Macdonald, K. C. Mid-Ocean Ridges: Fine Scale Tectonic, Volcanic and Hydrothermal Processes Within the Plate Boundary Zone. *Annual Review of Earth and Planetary Sciences* **10**, 155-190, doi:10.1146/annurev.ea.10.050182.001103 (1982).

2 Smith, D. K., Tivey, M. A., Schouten, H. & Cann, J. R. Locating the spreading axis along 80 km of the Mid-Atlantic Ridge south of the Atlantis Transform. *Journal of Geophysical Research: Solid Earth* **104**, 7599-7612, doi:10.1029/1998JB900064 (1999).

3 Ballard, R. D., Francheteau, J., Juteau, T., Rangan, C. & Normark, W. East Pacific rise at 21°N: The volcanic, tectonic, and hydrothermal processes of the central axis. *Earth and Planetary Science Letters* **55**, 1-10, doi:10.1016/0012-821X(81)90081-9 (1981).

4 Delaney, J. R. *et al.* The Quantum Event of Oceanic Crustal Accretion: Impacts of Diking at Mid-Ocean Ridges. *Science* **281**, 222-230, doi:10.1126/science.281.5374.222 (1998).

5 Mitchell, N. C. Characterising the extent of volcanism at the Galapagos Spreading Centre using Deep Tow sediment profiler records. *Earth and Planetary Science Letters* **134**, 459-472, doi:10.1016/0012-821X(95)00132-V (1995).

6 Dick, H. J. B., Lin, J. & Schouten, H. An ultraslow-spreading class of ocean ridge. *Nature* **426**, 405-412 (2003).

7 Smith, D. K. & Cann, J. R. Building the crust at the Mid-Atlantic Ridge. *Nature* **365**, 707-715, doi:10.1038/365707a0 (1993).

8 Smith, D. K. & Cann, J. R. Hundreds of small volcanoes on the median valley floor of the Mid-Atlantic Ridge at 24–30° N. *Nature* **348**, 152-155, doi:10.1038/348152a0 (1990).

9 Baines, A. G. *et al.* SHRIMP Pb/U zircon ages constrain gabbroic crustal accretion at Atlantis Bank on the ultraslow-spreading Southwest Indian Ridge. *Earth and Planetary Science Letters* **287**, 540-550, doi:10.1016/j.epsl.2009.09.002 (2009).

10 Schwartz, J. J. *et al.* Dating the Growth of Oceanic Crust at a Slow-Spreading Ridge. *Science* **310**, 654-657, doi:10.1126/science.1116349 (2005).

11 Rioux, M. *et al.* Protracted timescales of lower crustal growth at the fast-spreading East Pacific Rise. *Nature Geoscience* **5**, 275-278, doi:10.1038/ngeo1378 (2012).

12 Lissenberg, C. J., Rioux, M., Shimizu, N., Bowring, S. A. & Mével, C. Zircon Dating of Oceanic Crustal Accretion. *Science* **323**, 1048-1050, doi:10.1126/science.1167330 (2009).

13 Rioux, M., Cheadle, M. J., John, B. E. & Bowring, S. A. The temporal and spatial distribution of magmatism during lower crustal accretion at an ultraslow-spreading ridge: High-precision U–Pb zircon dating of ODP Holes 735B and 1105A, Atlantis Bank, Southwest Indian Ridge. *Earth and Planetary Science Letters* **449**, 395-406, doi:10.1016/j.epsl.2016.05.047 (2016).

14 Sturm, M. E., Goldstein, S. J., Klein, E. M., Karson, J. A. & Murrell, M. T. Uranium-series age constraints on lavas from the axial valley of the Mid-Atlantic Ridge, MARK area. *Earth and Planetary Science Letters* **181**, 61-70, doi:10.1016/S0012-821X(00)00177-1 (2000).

15 Standish, J. J. & Sims, K. W. W. Young off-axis volcanism along the ultraslow-spreading Southwest Indian Ridge. *Nature Geoscience* **3**, 286-292, doi:10.1038/ngeo824 (2010).

16 Clague, D. A. *et al.* Eruptive and tectonic history of the Endeavour Segment, Juan de Fuca Ridge, based on AUV mapping data and lava flow ages. *Geochemistry, Geophysics, Geosystems* **15**, 3364-3391 (2014).

17 Clague, D. A. *et al.* Geologic history of the summit of Axial Seamount, Juan de Fuca Ridge. *Geochemistry, Geophysics, Geosystems* **14**, 4403-4443 (2013).

18 Müller, R. D., Sdrolias, M., Gaina, C. & Roest, W. R. Age, spreading rates, and spreading asymmetry of the world's ocean crust. *Geochemistry, Geophysics, Geosystems* **9** (2008).

19 Klingelhöfer, F., Géli, L., Matias, L., Steinsland, N. & Mohr, J. Crustal structure of a super-slow spreading centre:a seismic refraction study of Mohns Ridge, 72° N. *Geophysical Journal International* **141**, 509-526, doi:10.1046/j.1365-246x.2000.00098.x (2000).

20 Carbotte, S. M., Smith, D. K., Cannat, M. & Klein, E. M. Tectonic and magmatic segmentation of the Global Ocean Ridge System: a synthesis of observations. *Geological Society, London, Special Publications* **420**, 249-295, doi:10.1144/sp420.5 (2016).

21 Cannat, M., Rommevaux-Jestin, C. & Fujimoto, H. Melt supply variations to a magma-poor ultra-slow spreading ridge (Southwest Indian Ridge 61° to 69° E). *Geochemistry, Geophysics, Geosystems* **4** (2003).

22 Dick, H. J., Lin, J. & Schouten, H. An ultraslow-spreading class of ocean ridge. *Nature* **426**, 405 (2003).

23 Dauteuil, O. & Brun, J.-P. Oblique rifting in a slow-spreading ridge. *Nature* **361**, 145 (1993).

24 Marks, N. S. Sedimentation on new ocean crust: The Mid-Atlantic Ridge at 37°N. *Marine Geology* **43**, 65-82, doi:10.1016/0025-3227(81)90129-8 (1981).

25 Smith, D. K. & Cann, J. R. The role of seamount volcanism in crustal construction at the Mid-Atlantic Ridge (24°–30° N). *Journal of Geophysical Research: Solid Earth* **97**, 1645-1658 (1992).

26 Chen, J., Cannat, M., Tao, C., Sauter, D. & Munschy, M. 780 Thousand Years of Upper-Crustal Construction at a Melt-Rich Segment of the Ultraslow Spreading Southwest Indian Ridge 50° 28' E. *Journal of Geophysical Research: Solid Earth* **126**, e2021JB022152 (2021).

27 Cannat, M. How thick is the magmatic crust at slow spreading oceanic ridges? *Journal of Geophysical Research: Solid Earth* **101**, 2847-2857 (1996).

28 Pedersen, R. B. *et al.* Discovery of a black smoker vent field and vent fauna at the Arctic Mid-Ocean Ridge. *Nat Commun* **1**, 126 (2010).

29 German, C. R. *et al.* Diverse styles of submarine venting on the ultraslow spreading Mid-Cayman Rise. *Proceedings of the National Academy of Sciences* **107**, 14020-14025, doi:10.1073/pnas.1009205107 (2010).

30 Tao, C. *et al.* First active hydrothermal vents on an ultraslow-spreading center: Southwest Indian Ridge. *Geology* **40**, 47-50, doi:10.1130/g32389.1 (2012).

31 German, C. R., Baker, E. T., Mevel, C., Tamaki, K. & the, F. S. T. Hydrothermal activity along the southwest Indian ridge. *Nature* **395**, 490-493, doi:10.1038/26730 (1998).

32 Edmonds, H. *et al.* Discovery of abundant hydrothermal venting on the ultraslow-spreading Gakkel ridge in the Arctic Ocean. *Nature* **421**, 252-256 (2003).

33 Michael, P. *et al.* Magmatic and amagmatic seafloor generation at the ultraslow-spreading Gakkel ridge, Arctic Ocean. *Nature* **423**, 956 (2003).

34 German, C. R., Petersen, S. & Hannington, M. D. Hydrothermal exploration of mid-ocean ridges: where might the largest sulfide deposits be forming? *Chemical Geology* **420**, 114-126 (2016).

35 Kinsey, J. C. & German, C. R. Sustained volcanically-hosted venting at ultraslow ridges: Piccard hydrothermal field, Mid-Cayman Rise. *Earth and Planetary Science Letters* **380**, 162-168 (2013).

36 German, C. R. *et al.* Volcanically hosted venting with indications of ultramafic influence at Aurora hydrothermal field on Gakkel Ridge. *Nature Communications* **13**, 6517, doi:10.1038/s41467-022-34014-0 (2022).

37 Macdonald, K. C. Mid-ocean ridges: Fine scale tectonic, volcanic and hydrothermal processes within the plate boundary zone. *Annual Review of Earth and Planetary Sciences* **10**, 155 (1982).

38 Perfit, M. R. & Chadwick, W. W. Magmatism at mid-ocean ridges: Constraints from volcanological and geochemical investigations. *Geophysical Monograph-American Geophysical Union* **106**, 59-116 (1998).

Supplementary Files

This is a list of supplementary files associated with this preprint. Click to download.

- SupplementaryInformation.pdf